






## RESEARCH ARTICLE

WILEY

# Ice wedge polygon stability on steep slopes in West Greenland related to temperature and moisture dynamics of the active layer

Katharina Schwarzkopf<sup>1</sup>  | Steffen Seitz<sup>1</sup>  | Michael Fritz<sup>2</sup>  |  
Thomas Scholten<sup>1</sup>  | Peter Kühn<sup>1</sup> 

<sup>1</sup>Soil Science and Geomorphology,  
Department of Geosciences, University of  
Tübingen, Tübingen, Germany

<sup>2</sup>Permafrost Research Unit, Alfred Wegener  
Institute, Helmholtz Centre for Polar and  
Marine Research, Potsdam, Germany

## Correspondence

Peter Kühn, Soil Science and Geomorphology,  
Department of Geosciences, University of  
Tübingen, Rümelinstr. 19-23, 72070.  
Tübingen, Germany.  
Email: [peter.kuehn@uni-tuebingen.de](mailto:peter.kuehn@uni-tuebingen.de)

## Abstract

Ice wedge polygons on steep slopes have generally been described as being covered by periglacial sediments and, typically, the active layer on slopes becomes mobile during thaw periods, which can lead to solifluction. In West Greenland close to the ice margin, however, the active layer and ice wedge polygons are stable despite their occurrence on steep slopes with inclinations of  $\geq 30^\circ$ . We conducted a soil survey (including sampling for soil analyses and radiocarbon dating) in the Umimmalissuaq valley and installed a field station  $\sim 4$  km east of the current ice margin to monitor soil temperature and water tension at depths of 10, 20 and 35 cm of the active layer on a steep, north-facing slope in the middle of an ice wedge polygon from 2009 to 2015. Thawing and freezing periods lasted between 2 and 3 months and the active layer was usually completely frozen from November to April. We observed simultaneous and complete water saturation at all three depths of the active layer in one summer for 1 day. The amount of water in the active layer apparently was not enough to trigger solifluction during the summer thaw, even at slope inclinations above  $30^\circ$ . In addition, the dense shrub tundra absorbs most of the water during periods between thawing and freezing, which further stabilizes the slope. This process, together with the dry and continental climate caused by katabatic winds combined with no or limited frost heave, plays a crucial role in determining the stability of these slopes and can explain the presence of large-scale stable ice wedge polygon networks in organic matter-rich permafrost, which is about 5,000 years old. This study underlines the importance of soil hydrodynamics and local climate regime for landscape stability and differing intensities of solifluction processes in areas with strong geomorphological gradients and rising air temperatures.

## KEYWORDS

permafrost, soil temperature, soil water tension, solifluction

This is an open access article under the terms of the [Creative Commons Attribution-NonCommercial-NoDerivs](https://creativecommons.org/licenses/by-nc-nd/4.0/) License, which permits use and distribution in any medium, provided the original work is properly cited, the use is non-commercial and no modifications or adaptations are made.

© 2023 The Authors. *Permafrost and Periglacial Processes* published by John Wiley & Sons Ltd.

## 1 | INTRODUCTION

During the 20th century, the rise of temperatures in the Arctic regions has been twice as strong as increases in the global average surface air temperature.<sup>1</sup> This affects the thawing of permafrost soils, which are sensitive to changing environmental conditions.<sup>2,3</sup> The abrupt thawing of permafrost and melting of the Greenland Ice Sheet are among the most widely debated tipping points or large-scale climate discontinuities, where a change in the global average temperature can foster self-reinforcing reactions such as a release of carbon to the atmosphere from ancient and previously freeze-locked carbon stocks.<sup>4</sup> This might impact the global carbon budget increasing carbon release to the atmosphere, which could lead to additional temperature increases.<sup>2,3,5–7</sup> Degradation of permafrost soils has been recorded at more than 100 sites studied in both hemispheres.<sup>8</sup>

Ice wedges are typically located near the top of the permafrost and are a widespread periglacial phenomenon in the circum-Arctic. They are formed by thermal contraction of the soil during winter.<sup>9,10</sup> In spring, meltwater infiltrates the cracks and re-freezes to form ice veins. Ice wedges are formed by repeated cracking over decades to millennia<sup>10,11</sup> and the formation of ice wedges leads to the typical polygonal patterns observed at the surface in Arctic landscapes.<sup>12</sup> In West Greenland, ice wedge polygons can be found on steep north-facing slopes. Ice wedge polygons on slopes in Antarctica<sup>13,14</sup> and Alaska<sup>15,16</sup> have been typically observed as being covered by periglacial sediments, which is not the case in West Greenland, where they are easily detectable and still widely distributed close to the ice margin of the Greenland Ice Sheet. Stable ice wedge polygons on steep slopes not overlain by solifluction layers have so far only been described by Sørbel and Tolgensbakk<sup>17</sup> on Spitsbergen. Therefore, this can be considered as an exceptional phenomenon on steep slopes where the surface expression of the underlying anti-syngenetic ice wedges is usually obscured.<sup>9</sup> Anti-syngenetic ice wedges are defined by growing on denudation slopes or in areas with ground-surface lowering by net removal of active-layer material, by erosion, or by mass movement.<sup>15,16</sup>

The development of stable ice wedge polygons on slopes has rarely been studied and only a few effects of water tension on the stability of the active layer are known. The active layer usually becomes mobile on slopes during thawing periods, which can lead to solifluction at low pF-values (logarithm of the soil water tension) or even active-layer detachments.<sup>18</sup> Solifluction is described as slope failures associated with the action of freeze–thaw that is reflected in a flow over a shear plane.<sup>19</sup> The occurrence of solifluction in periglacial areas generally depends on the inclination, soil temperature and soil moisture content of the active layer.<sup>20</sup> In West Greenland, however, the active layer is stable on most north-facing slopes with inclinations of 30° on average.<sup>21</sup>

Therefore, we hypothesize that the active layer on steep slopes near the ice margin in West Greenland is stable because the water tension at low pF-values in the active layer is not high enough to trigger solifluction during freeze–thaw cycles. To test this hypothesis, we installed sensors for soil water tension and soil temperature within

the active layer in the middle of an ice wedge. In connection with the stability of the active layer on these steep slopes, we evaluated ice wedge polygon stability by analyzing additional data on soil properties and radiocarbon dates of organic material from the organic matter-rich permafrost of these slopes in which the ice wedges have formed.

## 2 | MATERIAL AND METHODS

The study area is located in the Umimallissuaq valley on a north-facing, exposed hillside with an incline of 33°, about 28 km southeast of Kangerlussuaq (see Figure 1) and is in an area with a continuous permafrost regime.<sup>22</sup> The climate in Kangerlussuaq, which is located 130 km inland from the west coast, is determined by its location in a 2- to 3-km-wide valley surrounded by mountains. From the northeast, the Greenland Ice Sheet has a significant influence on precipitation and winds, resulting in a Low Arctic continental climate, Arctic Bioclimate Zone E<sup>23</sup> with temperatures about –40°C in the winter months and 18°C in the summer months. The average annual temperature is –5.7°C and the average annual precipitation is 150 mm (Danish Meteorological Institute, 1977–1999). The study area in the Umimallissuaq valley is strongly affected by katabatic winds from the Greenland Ice Sheet. The wind direction is mainly northeast with a mean wind speed of 3.6 m s<sup>–1</sup> and a maximum wind speed of 19.6 m s<sup>–1</sup>.<sup>24</sup> In comparison, Nuuk, on the southwestern coast of Greenland, has an average annual temperature of –1.2°C and an annual precipitation of 750 mm (Danish Meteorological Institute, 1977–1999). These coastal areas have a greater maritime influence with higher precipitation and higher temperatures.

The Umimallissuaq valley lies within the Umîvît/Keglen moraines, which were deposited 8.05 ± 0.17 ka<sup>25</sup> and run mainly north to south through the valley with well-defined ridges. From the area within these moraines the oldest radiocarbon age of organic matter in the Sandflugtdalen is from gyttja (subhydric soil in well-aerated, nutrient-rich waters consisting of fine mineral material mixed with organic matter) and gave an age of about 7,300 cal BP for UtC-1987.<sup>26</sup> The radiocarbon age from the basal gyttja in the Lille Saltsø, situated about 10 km to the southwest of UtC-1987, gave an age of about 8,050 cal BP for AAR-3507.<sup>27</sup> This means that deglaciation started about 8,000 years ago and thus also gives a maximum age for the formation of periglacial phenomena.

Although situated in the area of continuous permafrost, the soils show characteristics of a discontinuous permafrost regime depending on their topographic position. On north-facing slopes, permafrost is present within the first 100 cm. The depth of the active layer varies across the valley and could not be reached in the valley bottom or on south-facing slopes.<sup>21</sup> Cryosols show faint cryogenic properties such as cryoturbation and sorting. Most Turbic Regosols and Cryosols occur in the moist valley, while at dry crest positions Turbic Regosols and Cryosols without turbic properties dominate. Periglacial phenomena and patterned ground are widespread, including ice wedge polygons on north-facing slopes and ice wedge pseudomorphs and earth hummocks on the valley floor. Solifluction phenomena occur very

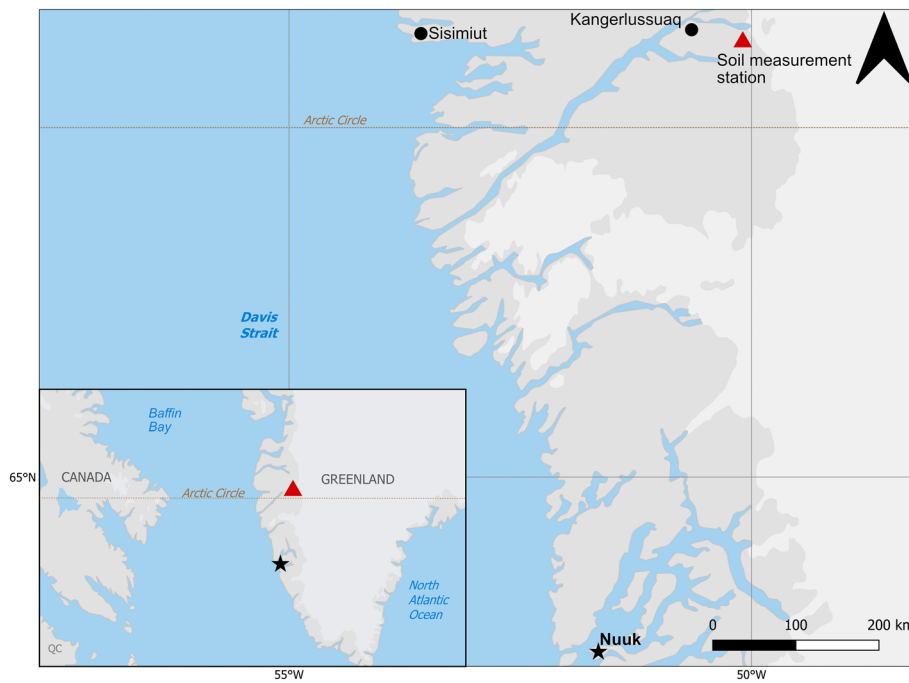


**FIGURE 1** Map of West Greenland with the capitol city Nuuk and Kangerlussuaq about 28 km northwest of the soil measurement station in the Ummimalissuaq valley.

rarely at the footslopes of north-facing slopes.<sup>21,24</sup> Due to the katabatic winds, areas of sediment erosion or deflation are mainly oriented eastward, while the areas of deposition are oriented seaward along the Ummimalissuaq valley. Müller et al.<sup>24</sup> described eolian layers based on grain size analyses of about 40 profiles along four Catenae in the Ummimalissuaq valley, with the grain sizes of the eolian layers becoming finer with increasing distance from the ice margin. Many Ahb horizons in the Ummimalissuaq valley are covered by eolian sediments.

To observe the behavior of soil temperature and soil water retention during thaw and freeze periods, an active layer monitoring station was installed on a north-facing slope in the Ummimalissuaq valley.

The monitoring station was positioned in the middle of an ice wedge polygon (profile C12 in Figure 2) to obtain direct information on seasonal and annual variation of soil temperature regime and water retention in the active layer in close relation to polygon development. The combined temperature and pF-sensors (soil-moisture tension; ecoTech Umwelt-Meßsysteme GmbH, Bonn, Germany) were installed at depths of 10 cm (pF<sub>1</sub>-sensor), 20 cm (pF<sub>2</sub>-sensor), and 35 cm (pF<sub>3</sub>-sensor). Water tension is typically given as the pF-value ranging from pF 1 (fast moving seepage water) to pF 4.2 (dry, not plant-available adhesive water) with pF 0 stating full water saturation or field capacity. Converted, these values represent  $-10^1$  hPa (pF 1),  $-10^{4.2}$  hPa (pF 4.2) and  $-1$  hPa (pF 0).<sup>28</sup> Water tension is usually measured in hPa or in centimeters of water column. Because of the wide range of values (0 to 10 million hPa), the measured values are automatically logarithmized and then expressed as a pF-value. Data collection began on August 5, 2009 and ended on July 6, 2015. Data were collected hourly and sent to a data logger. The pF<sub>1</sub>-sensor at 10 cm depth failed on July 27, 2012 and could not be reinitiated.



**FIGURE 2** Steep north-facing slope with two ice wedge polygon nets. The arrow shows the location of the monitoring station in the middle of an ice wedge polygon on a 33° slope.

Fieldwork was carried out every summer between July and August from 2009 to 2015. Bulk samples for soil analyses and additional bulk soil organic material for radiocarbon dating were collected from soil pits in 2009 (see Figure 3 for the location of the pits). The monitoring station was installed in August 2009 and had to be maintained every summer until 2015 for battery replacement. The soil profiles were described and classified according to the World Reference Base for Soil Resources (IUSS Working Group 2022).

The monitoring data for this study were analyzed from the beginning of the thawing period until the freezing period, since this time range has the highest water saturation. We defined the annual period of thawing of the active layer, from soil  $t > 0^\circ\text{C}$  at a depth of 10 cm, to soil  $t > 0^\circ\text{C}$  at a depth of 35 cm. If the active layer did not thaw to a depth 35 cm in any one year, the thawing period was defined as

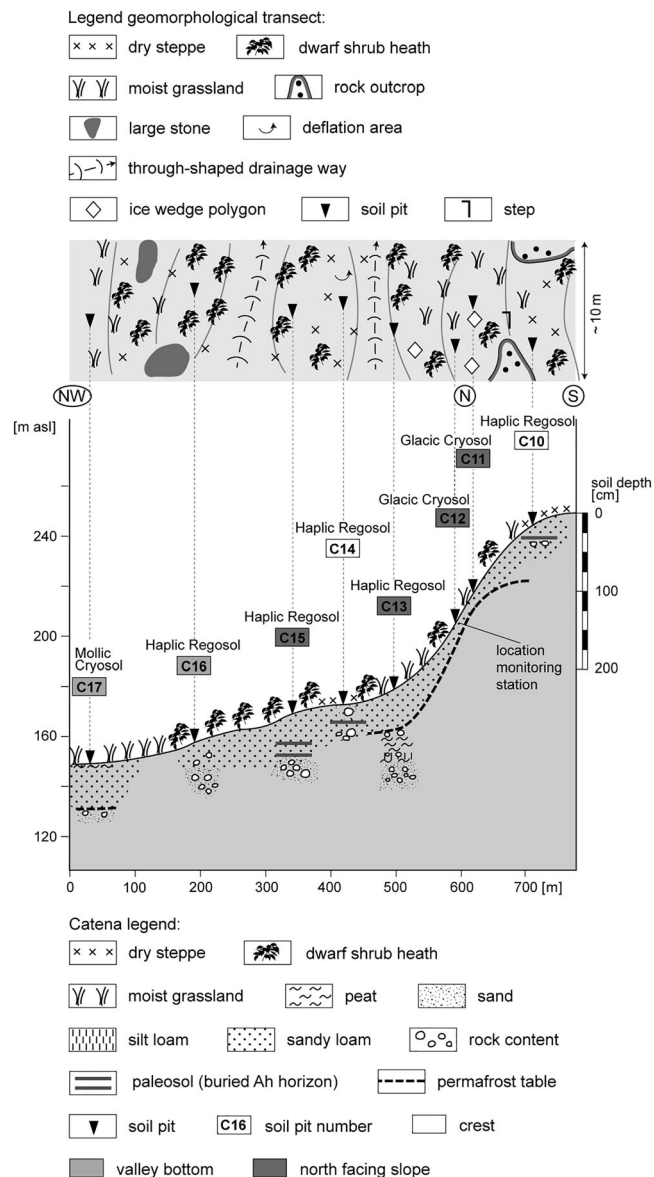


**FIGURE 3** Transect and catena in the Ummimalissua valley about 4.5 km west of the ice margin. Reference soil groups are after the IUSS WRB Working Group (2022).<sup>75</sup> The active layer was mapped with a 1-m ice probe. Modified from Henkner et al.<sup>21</sup>

when the soil had  $t > 0^{\circ}\text{C}$  at a depth of 20 cm. The freezing period was defined as when the soil had  $t < 0^{\circ}\text{C}$  at 10 cm until the time when the entire active layer was completely frozen, as the pF<sub>3</sub>-sensor was installed at a depth of 35 cm directly above the permafrost table. Graphs were produced with QGIS (QGIS Geographic Information System; QGIS Association), the Software R (R Core Team 2017) with the packages ggplot2<sup>29</sup> and tidyverse,<sup>30</sup> and with Surfer based on Kriging Interpolation from Golden Software (LLC).

An elemental analyser (“Vario EL III”, Elementar Analysensysteme GmbH, Germany, in CNS mode) with helium atmosphere and oxidative heat combustion at 1150°C was used to measure total carbon and nitrogen content by dry mass. Since the soil-pH<sub>[CaCl<sub>2</sub>]</sub> values are about 5.5 and there is no source of inorganic carbon in the study

area,<sup>31</sup> we assumed that total carbon is equal to SOC (soil organic carbon). Soil-pH (0.01 M CaCl<sub>2</sub>) was analysed with a Sentix 81 (WTW, pH340) using a soil to solution ratio of 1:2.5.<sup>28</sup>

Two samples of bulk SOC from permafrost in profile C11 were taken for radiocarbon dating. Calibration of the accelerator mass spectrometry (AMS) <sup>14</sup>C ages to calendar years was done with OxCal 4.4.4 using the IntCal20 calibration curve.<sup>32,33</sup> Radiocarbon dating was performed after pre-treatment using the acid-alkali-acid method: samples were first heated at 80°C in 1 M HCl to remove carbonates. Then, the samples were heated at 80°C in 1 M NaOH to remove humic acids and fulvic acids. Afterwards, the samples were heated at 80°C again in 1 M HCl to remove remaining carbonates. Finally, the samples were dried at 100°C and stored in closed glasses to avoid contamination.

### 3 | RESULTS

#### 3.1 | Soil carbon content, soil texture and AMS <sup>14</sup>C age

Compared to the other soils in the catena (Figure 3), the soils on the ridges (Regosols) have a lower SOC content with about 5% in the Ah horizon and <2% in the other horizons (see Table S1). The highest SOC content of about 10% occurs in soils with a shallow active layer (C12, C13) and within the permafrost on north-facing slopes, where organic matter-rich permafrost is present.

Silt content varies mostly from 50% to 65% with a generally low clay content of ≤8% in all horizons. Weak cryoturbation phenomena were only observed at the footslope in the upper 50 cm of C13 and in the valley floor bottom (C16, C17). Profiles C10–C17 were also part of cross-section 1 in Müller et al.<sup>24</sup> The eolian deposits of cross-section 1 are predominantly silt loam (Table S1 this study; figure 4c in Müller et al.<sup>24</sup>) and are responsible for the occurrence of buried A horizons on the upper slope (C10) and in the profiles at the transition from slope to the valley (C13, C14).

On the steep north-facing slopes, the characteristic vegetation is continuous dwarf shrub heath with *Betula nana*, *Salix glauca*, *Equisetum arvense*, *Rhododendron lapponicum*, Cyperaceae, mosses and herbs. Dry steppe communities with *S. glauca*, *Pyrola grandiflora*, *B. nana*, Poaceae, and forbs dominate on ridges and wind-exposed areas.<sup>21,34</sup>

The lowermost sample (Erl-16618) in profile C11 gave an age of the organic material of 3,481–3,230 cal BP at 200 cm depth (Table 1). The full depth extent of the permafrost was not reached. The age of MAL-12293 at 120 cm depth is about 800 years younger, if the age of 2,620–2,414 cal BP with the highest probability is taken.

#### 3.2 | Comparing the upper soil temperature of ice wedge polygons with air temperature of Kangerlussuaq

Air temperature was measured in the climate station in Kangerlussuaq (Figure 4, Data from the Danish Meteorological Institute).

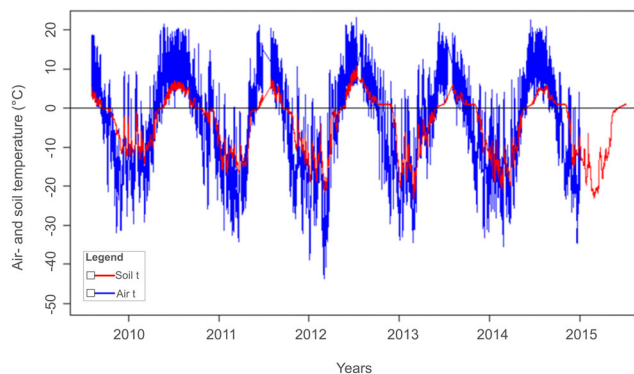
**TABLE 1** AMS  $^{14}\text{C}$  data related to the deglaciation of the Umimallissuaq valley. The data from Müller et al.<sup>24</sup> were supplemented with the original  $\delta^{13}\text{C}$  results.

Sampling location	Lab-no.	Horizon/layer	Depth (cm)	Calibrated age, 95.4% probability (cal BP) <sup>a</sup>	$^{14}\text{C}$ age (BP)	$\delta^{13}\text{C}$ (‰)	Material	Relevance (min./max. age)	Reference <sup>b</sup>
Sandflugtdalen (67.09°N/50.29°W)	UtC-1987	—	200	7,481–7,154 (88.8%) 7,124–7,017 (6.6%)	6,380 ± 100		Gyttja	Max. Ørkendalen moraines	Van Tatenhove et al. <sup>26</sup>
Lille Saltsø (66°59.3N, 50°38.6W)	AAR-3507	—	175–176	8,173–7,935	7,210 ± 60	−18.2	Clay gyttja	Min. Umivit/Keglen	Bennike <sup>27</sup>
C17 (valley floor)	Erl-19000	Ah (lowest part)	50	5,285–5,161 (29.5%) 5,142–4,869 (66.0%)	4,433 ± 54	−27.3	Soil organic material	Min. Umivit/Keglen, max. Ørkendalen moraines	Müller et al. <sup>24</sup>
C33 (between footslope and lateral moraine, buried by glaciofluvial sediments)	Erl-16614	Ahb	60–62	4,826–4,518 (92.2%) 4,470–4,448 (3.3%)	4,114 ± 53	−26.7	Soil organic material	Min. Umivit/Keglen, max. Ørkendalen moraines	Müller et al. <sup>24</sup>
C11 (slope)	MAL 12293	Permafrost	120	2,707–2,627 (35.1%) 2,620–2,414 (58.6%) 2,385–2,371 (1.7%)	2,465 ± 22	−21.3	Soil organic material	Accumulation of organic-rich permafrost	This study
C11 (slope)	Erl-16618	Permafrost	200	3,481–3,230	3,158 ± 56	−26.8	Soil organic material	Accumulation of organic-rich permafrost	This study

<sup>a</sup>Calibration was carried out with OxCal v 4.4.4 (Bronk Ramsey<sup>32</sup>); atmospheric are data from Reimer.<sup>33</sup>

<sup>b</sup>The listed radiocarbon ages are crucial for the discussion of the onset of formation of periglacial features in the study area.

Despite a distance of 28 km between the two measuring stations, the soil temperature curve at 10 cm depth of the measuring station behaved similarly to the air temperature curve but with a smaller range of values. Over the period monitored, there were maximum air temperature values of 23.3°C (2012, July 10) and minimum temperatures of −43.3°C (2012, March 1). The amplitude of soil temperature was much smaller, with extreme values ranging from a maximum of 10.9°C (2012, July 9) to a minimum of −23.2°C (2013, February 26) and diurnal variability of air temperature was also higher than diurnal variability of soil temperatures. In the winters 2009/2010, 2012/2013, and 2013/2014 there were frequent positive air temperatures; at the same time, soil temperatures also increased, but never exceeded 0°C. It became clear that the soil temperature acted similarly to the air temperature, usually with a time delay of 12–24 h. For example, the data showed that

**FIGURE 4** Annual air and soil temperatures 2009–2015 at 10 cm depth (after Beutelspacher<sup>35</sup>).

in November 2010 maximum air temperature was 3.8°C (2010, November 6, 2:00 a.m.). Just 13 h later (2010, November 6, 3:00 pm) a maximum soil temperature of -0.48°C was recorded. It can be assumed that the soil temperature curves at 20 and 35 cm depth reacted similarly but with a lower amplitude and a time delay of on average 12 h in the thawing period and 6 h during the freezing period.

### 3.3 | Freezing periods

The freezing periods showed comparable behavior every year: as the air temperature decreased below 0°C for the first time every year between September 15 and 20 (except in 2013, when negative temperature values occurred on August 19), the soil temperature also dropped with a time delay of 12–24 h and the active layer froze from the bottom up. In each year, the soil temperature at 20 and 35 cm depth had already dropped at the beginning of the freezing phase. If it was not already below 0°C, the temperature at 35 cm fell below 0°C within the first week of the freezing period. Between 10 and 20 days after the soil temperature dropped below 0°C at 35 cm depth, the soil temperature at 20 cm dropped below 0°C for the first time, but fluctuations still occurred, as observed in every year, except in 2011 and 2014. After 4–6 weeks (except in 2012, when it took 8 weeks), the soil temperature at 10 cm depth showed negative values for the first time. Re-freezing (Figure 5) began between mid-August and early September and ended in early November, with the exception of 2012, when the active layer was not completely frozen until December. The longest freezing periods were recorded in 2012 and 2013, of about 100 and 90 days respectively, while in 2009, 2010, and 2014 this process lasted between 60 and 70 days. In 2011, the active layer was completely frozen after only 40 days.

In 2009–2011 the lowermost instrumented soil depth at 35 cm did not reach positive temperature values over the summer months. Overall, it is notable that soil temperatures dropped below 0°C distinctly faster in 2009–2011, within 7 and 33 days, than in the following years, between 59 and 106 days in 2012–2014. However, as soon as temperatures dropped below 0°C, they decreased more consistently than in the three winters from 2009 to 2011.

In contrast, the pF-values differed every year (Figure 5). Strikingly, there were long periods of complete water saturation in the lowest part of the active layer in every year except 2011, varying from 1 week as in 2009 or almost the entire freezing period as in the other years observed. The pF-values only increased again once the soil temperature fell below 0°C. Interestingly, variations in water tension occurred despite a soil temperature below 0°C. The years 2009–2011 clearly show that although the active layer at the lowest depth showed no temperature values >0°C, fluctuations in water tension occurred. However, as soon as the soil temperature was well below 0°C, around -3°C, the pF-values also increased strongly. The highest values (pF > 3) of the freezing periods were measured at the end, which

marked the time the soil was completely frozen and the water tension was thus at its highest.

### 3.4 | Thawing periods

The thawing period (Figure 6) started in May and ended in July each year. The active layer thawed from the top down to 35 cm within 63 days in the years 2010, 2011, and 2012. In the following years, thawing was 6 days faster in 2013 and 7 days faster in 2014. Soil temperatures at all three depths in every year responded to variations in the same way, with only a slight delay of 2–3 weeks (2011, 2012), 4 weeks (2010, 2015), and 6 weeks (2013, 2014). The active layer at 10 cm depth had the longest unfrozen periods and the active layer at 35 cm depth showed the shortest periods with temperatures above 0°C.

As seen during the freezing period, pF-values varied strongly across the thawing periods and from year to year. However, it is notable that at the beginning of the thawing period the pF-values were high (pF > 4). Over the course of the thawing period and with rising soil temperatures, the water tension decreased. This process, similar to soil temperature, began in the upper soil depth and proceeded downward within a time delay of 2–3 weeks. In contrast to the freezing period, which showed several freezing cycles, every thawing period is characterized by one continuous downward thaw. There are no fluctuations around 0°C temperature. As soon as the soil temperature reached positive values at a depth of 10 cm, the water tension at this depth dropped to pF = 0 in 2010, 2011, and 2012. Notably, in every year, between the beginning and middle of June, there was a rapid drop in water tension to pF = 0 within 1–2 days in at least one active layer depth.

### 3.5 | Water tension in the active layer

Water tension between pF = 0 (soil fully saturated) and the upper limit of capacity at pF = 1.8 did not occur at the same point in time when comparing the three soil depth layers (Table 2). In the freezing periods of 2009 and 2011 (Figure 5) and in the thawing periods of 2010, 2011, 2013, 2014, and 2015 (Figure 6), there was no simultaneous decrease in water tension to pF < 1.8 in the whole active layer. There were periods when individual depths experienced complete water saturation for several hours, but never all at the same time. However, in every freezing period except for 2011, as well as in the thawing period of 2012, there was a temporal overlap (a simultaneous water tension of pF < 1.8 or pF = 0 at all measured depths) of pF-values < 1.8 at all three depths, or from mid-2012 at the lower two depths. Lower water tension occurred at the respective depths for 55 days (2010), 18 days (2012 thaw period), 99 days (2012 freeze period), 85.5 days (2013), and 55 days (2014). Crucially, these periods refer only to an overlap of pF < 1.8 but not pF > 0. There was simultaneous complete water saturation (pF = 0) at 20 and 35 cm depth only from October 13 to 14 in 2013 for 25 h.

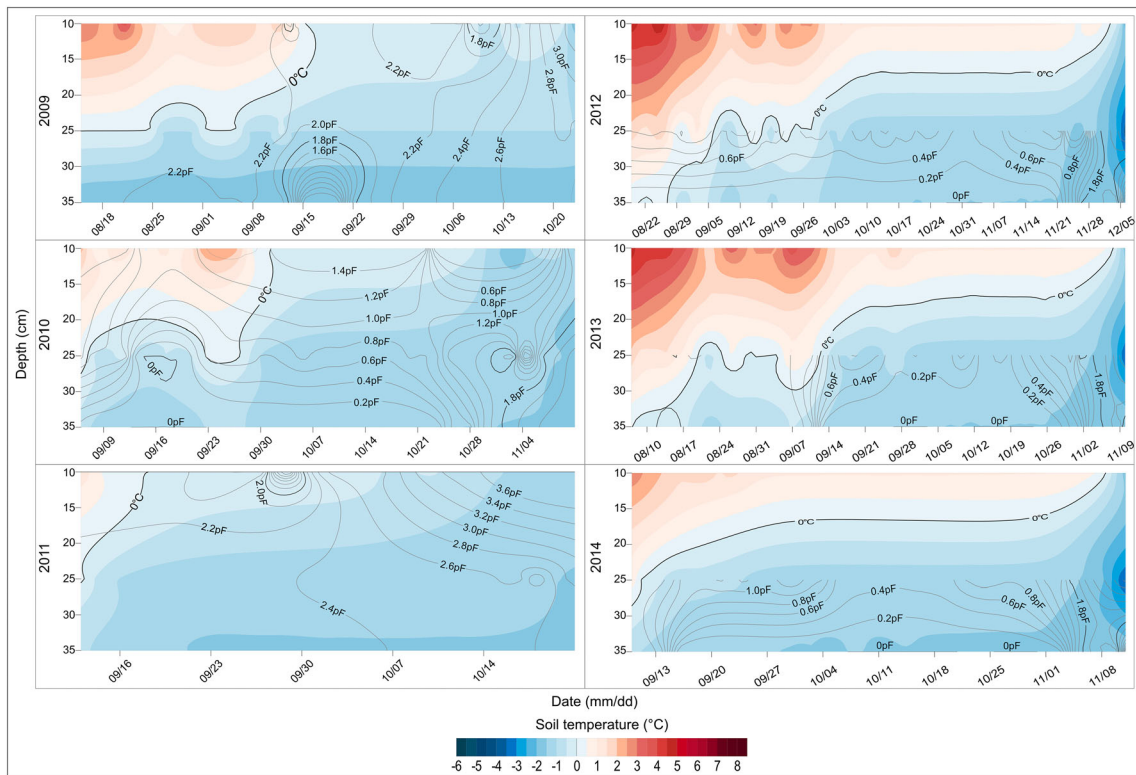


**FIGURE 5** Soil temperature and pF-values during freezing periods from 2009 to 2014. The temperature change is shown using colors (red and blue) and the variation of soil moisture tension is drawn using lines.

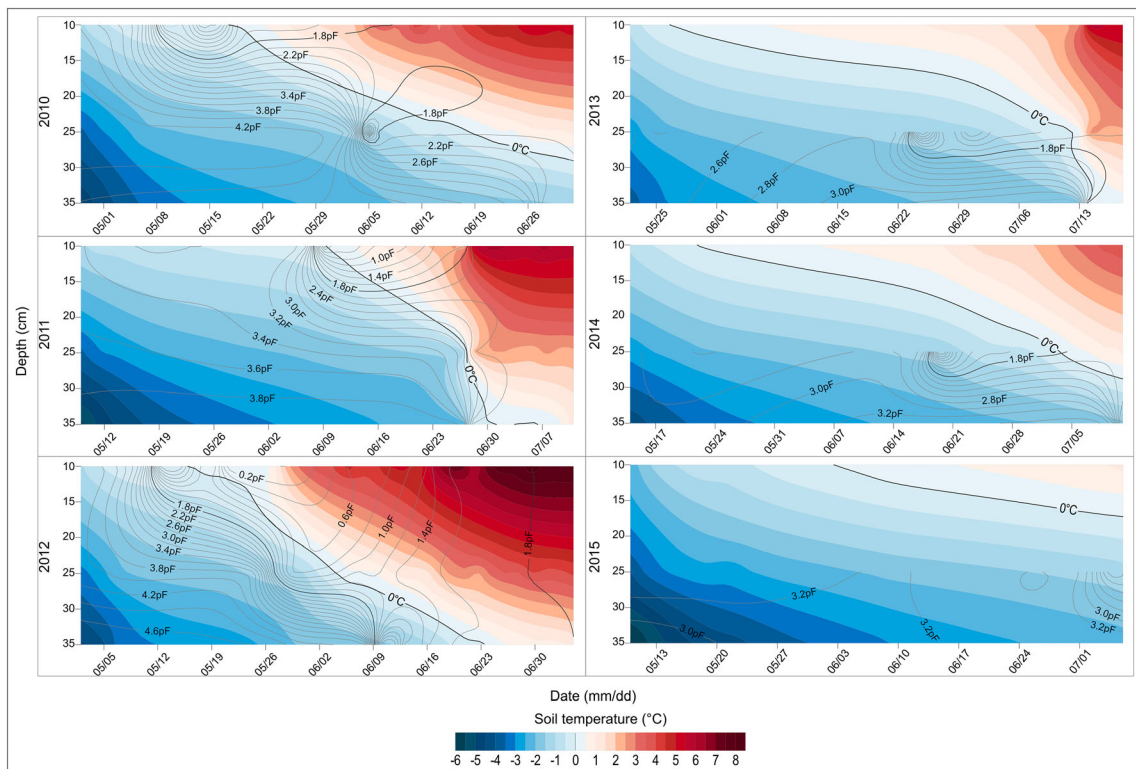


**FIGURE 6** Soil temperature and pF-values during thawing periods from 2010 to 2015. The temperature change is shown using colors (red and blue) and the variation of soil moisture tension is drawn using lines.

**TABLE 2** State of water saturation (pF-values <1.8 and 0) at three depths of the active layer from 2009 to 2015 with time periods when the pF values overlap at the investigated depths.

	10 cm	20 cm	35 cm	Overlapping periods of pF < 1.8 or pF = 0 (in hours) at all depths
<b>2009</b>				
<b>Freezing period</b>				
pF < 1.8 in hours	111	0	213	No overlap
pF = 0 in hours	20	0	156	No overlap
<b>2010</b>				
<b>Thawing period</b>				
pF < 1.8 in hours	697	37	0	No overlap
pF = 0 in hours	34	21	0	No overlap
	11			
	5			
<b>Freezing period</b>				
pF < 1.8 in hours	1,625	1,404	1,365	06.09 to 31.10 (1,328 h)
		76		
pF = 0 in hours	285	103	689	No overlap
	62	37	421	
		22		
<b>2011</b>				
<b>Thawing period</b>				
pF < 1.8 in hours	455	0	0	No overlap
pF = 0 in hours	31	0	0	No overlap
<b>Freezing period</b>				
pF < 1.8 in hours	54	0	0	No overlap
pF = 0 in hours	32	0	0	No overlap
<b>2012</b>				
<b>Thawing period</b>				
pF < 1.8 in hours	1,174	791	502	09.06 to 29.06 (474 h)
pF = 0 in hours	10	0	68	No overlap
	73			
	31			
	176			
<b>Freezing period</b>				
pF < 1.8 in hours	NA	2,493	2,384	19.08 to 26.11 (2,384 h)
pF = 0 in hours	NA	107	2,204	No overlap
<b>2013</b>				
<b>Thawing period</b>				
pF < 1.8 in hours	NA	600	0	No overlap
pF = 0 in hours	NA	54	0	No overlap
<b>Freezing period</b>				
pF < 1.8 in hours	NA	161	2,179	17.08 to 01.11 (2,056 h)
		2,061		
pF = 0 in hours	NA	25	1,011	13.10 to 14.10 (25 h)
<b>2014</b>				
<b>Thawing period</b>				
pF < 1.8 in hours	NA	384	0	No overlap
pF = 0 in hours	NA	23	0	No overlap
<b>Freezing period</b>				
pF < 1.8 in hours	NA	1,317	1,370	10.09 to 03.11. (1,317 h)

(Continues)



TABLE 2 (Continued)

	10 cm	20 cm	35 cm	Overlapping periods of pF < 1.8 or pF = 0 (in hours) at all depths
pF = 0 in hours	NA	0	1,131	No overlap
<b>2015</b>				
<b>Thawing period</b>				
pF < 1.8 in hours	NA	11	0	No overlap
pF = 0 in hours	NA	0	0	No overlap

## 4 | DISCUSSION

### 4.1 | The role of soil moisture and soil temperature for slope stability

The soil water content in the active layer is decisive for the stability of a slope.<sup>19</sup> Increasing water saturation leads to both an increasing mass per unit soil volume and a loss of capillary rise. Both factors can trigger mass movements along slopes.<sup>36,37</sup> Seepage water in particular can trigger soil movements,<sup>38</sup> which is why the value of pF = 0 is crucial in this study and hence why the duration of water saturation at the respective depths was studied in more detail. Further, even if only shrubby vegetation is present, plants have a stabilizing influence on a slope,<sup>39,40</sup> which also is associated with soil moisture. Hydraulic and mechanical effects,<sup>41</sup> especially transpiration processes that keep the active layer in an unsaturated and drier state, can stabilize slopes.<sup>42</sup> Due to climate warming, shrub vegetation in Arctic areas has expanded in recent decades,<sup>43</sup> leading to diverse growth forms and seasonal water consumption as a result of different rooting depths.<sup>44</sup> *B. nana*, for example, relies on snow melt-water for 40% of its water uptake throughout the active layer.<sup>45</sup> At values of pF below 1.8, soil water is not held in the soil against gravity, but the water can still be absorbed by the plant roots. Therefore, the active layer is not affected strongly by gravitational movements. Only at complete water saturation (pF = 0), where the air content in the soil is zero,<sup>46</sup> does the soil experience viscous flow that exceeds the power of the roots to hold the soil against gravity, and the slope can start to move.

The freezing point of the soil water was assumed to be 0°C. Nevertheless, when analyzing the thawing and freezing periods, it was found that this assumption does not apply in our case. This is particularly crucial in the years 2009–2011, which showed no positive soil temperature values at 35 cm depth throughout the year, yet variations in water tension occurred. Since the water tension in soil pores is >4 when the active layer is frozen,<sup>47</sup> pF values <2 indicate the presence of unfrozen water and thus a freezing/melting point of this soil water of <0°C. There are various reasons for liquid water to be present in a freezing soil: (a) capillary forces, (b) adsorption forces, and (c) dissolved ions.<sup>48,49</sup> In our case, the sensors were installed at 10, 25, and 35 cm below the surface so the pressure gradient is not high enough. Moreover, although there are lakes with elevated salinity in the study area,<sup>50</sup> the measured EC in profile C11 is 269  $\mu\text{S cm}^{-1}$  so

salinity in this profile can also be excluded. Therefore, it is likely that the pore size distribution and thus the adsorption forces are responsible for freezing point depression.

### 4.2 | Freezing periods

Every fall/early winter (except in 2011), the soil moisture tension dropped below pF = 1.8 at 35 cm depth, even though the soil temperature showed negative values. Moreover, in every year, except 2011, there was a period of between 3 days (in 2009) and 1 or 2 months (in 2010, 2012, 2013, and 2014), where the sensor at 35 cm depth measured values of pF = 0. These periods of water saturation can be explained by the subsurface, downslope flow of water on the frozen transition zone.<sup>51</sup> Here, the permafrost table acted as a vertical barrier for flowing water, causing soil water to move downslope.<sup>52</sup> In addition, a temporal overlap of water tension pF > 1.8 occurred in each year, except 2011, for 55 days (2010), 99 days (2012), 85 days (2013), and 54 days (2014). At the time when the freezing periods began (late August/September), air temperature (Figure 4) and solar radiation decreased. Thus, there was less active plant growth and therefore less water was absorbed by the roots.<sup>53</sup> Consequently, more soil water accumulated in the active layer, explaining the longer periods of low water tension. Since there have been periods of continuous low water tension (pF > 1.8) in almost every year, but the ice wedges are nevertheless stable, pF = 0 seems to have a greater impact on the instability of the active layer than pF > 1.8 and therefore provides better conditions for solifluction. Prolonged periods of complete water saturation did occur at each depth, but with the exception of 2013, no overlap occurred at any time. It is possible that 25 h of pF = 0 at 20 and 35 cm depth in October 2013 (Table 2) was not long enough to trigger slope movement, or another decisive factor is that no data on the pF<sub>1</sub>-sensor are available. As soil movement can be excluded, and the active layer at 10 cm depth was not yet frozen at this time, it can be assumed that the pF<sub>1</sub>-values were >0.

As mentioned above, it was observed that pF-values increased above 4 throughout the active layer at the end of the freezing period as soon as soil temperature values were in the negative range (below –3°C). Thus, the soil was completely frozen (Figure 5). Sequentially, there was a stagnation of soil temperature in fall and early winter

every year after the rapid drop in air temperatures. This was caused by the insulation effect of snow cover on the surface.

### 4.3 | Thawing periods

As soon as the air temperature reached values between 4 and 8°C in mid-May/June, the active layer directly under the surface started to thaw. The active layer at 10 cm depth has the longest unfrozen periods and at 35 cm depth the shortest periods with temperature above 0°C. Moreover, the rising temperature in spring and early summer affected both the soil temperature and the soil moisture tension. During snowmelt, when evapotranspiration is lower and the vegetation is still inactive, the inflow of meltwater results in low soil suction and deeper water infiltration.<sup>54,55</sup> Rising temperatures in spring begin to melt the snow cover and thaw of ice in the soil pores starts, leading to increased water content in the active layer. In 2012 the pF<sub>3</sub>-sensor measured positive temperature values for the first time. Air temperature in summer 2012 reached its maximum at 23.3°C on July 10 (Figure 4). Compared to the previous summers, this one was particularly warm as 97% of the ice sheet in Greenland underwent surface melt.<sup>56</sup> As climate change progresses, it has also been noted that the thawing period has become shorter, which means that thawing of the active layer is faster, resulting in longer ice-free periods. In 1986–2000, thawing lasted on average until mid-August.<sup>8</sup> Compared to the present data, thawing of the active layer lasted only until early/mid-July and the active layer remained unfrozen until the beginning of the freezing period.

In 2010, 2011, and 2012 the soil moisture tension at 10 cm depth dropped directly to pF = 0 for 55 h with a short interruption (2010), for 31 h (2011), and for 73 h also with a short interruption (2012) once the temperature at this depth reached positive values. As soon as the active layer begins to thaw, the water content near the surface increases, and thus the water tension decreases.<sup>57,58</sup> According to our observations, the same happened in the following years but due to the failed pF<sub>1</sub>-sensor, no measurement-based data regarding the water content in this depth can be added. Overall, the thawing periods clearly show that the pF-value, which was always >4 at the beginning of this period, marking the frozen stage, only began to decrease when the soil temperature reached -2°C (Figure 6). Thus, it can be concluded that -2°C represents the freezing point of this active layer. Therefore, the water tension falls rapidly at 0°C, as the active layer has already been thawing for at least 2 weeks.

Accumulation of snowmelt and ice meltwater did result in increased water content in the active layer, but with the exception of 2012 (20 days with pF < 1.8), this did not occur simultaneously in all three layers. In particular, the active layer at 35 cm showed water tension values of <1.8 for 21 days only in 2012. The fact that 2012 is an exception could be due to the hot summer, which caused increased ice melt. It is possible, since the active layer also had positive temperature values for the first time at 35 cm that year, that the thickness of the active layer may have increased. However, the fact that the water

tension in the active layer did not decrease simultaneously may have alternative explanations. First, that the active layer reacted 2–3 weeks later at depths of 20 and 35 cm, respectively, thus shortening the conditions for simultaneous water saturation. Second, in late May/early June plant activity and thus water uptake by roots increases, which also resulted in less frequent simultaneous low water tension at all soil depths.<sup>53</sup> In addition, air temperatures reached an average of 12°C during the summer months (from mid-June to mid-August). This caused a decreasing amount of soil water,<sup>59</sup> exacerbated by the continental climate,<sup>24</sup> and thus it led to complete water saturation at 10 cm only in May (and in early June for 31 h in 2011).

### 4.4 | Causes of stable active layers on steep slopes

Since the soil measurement station was located on a slope with an inclination of 33°, it is very likely that repeated freezing and thawing cycles could cause gravitational mass movement such as solifluction.<sup>60</sup> Especially on periglacial slopes, solifluction is the most common slope-deforming process<sup>61</sup> and leads to ice wedge polygons being covered with sediments.<sup>16</sup> However, no movement was observed during the monitoring period. In addition, the presence of stable and visible ice wedge polygons indicates that there was no recent movement, either (Figure 2). In 2009, 2010 (thawing period), 2011, 2013 (thawing period), 2014 (thawing period), and in the short observation period of 2015 (Table 2), the conditions for solifluction were not ideal. Since the soil moisture content is one of the main factors for solifluction, the active layer has to be sufficiently saturated with water.<sup>19</sup> During those periods, the three layers were not saturated with water at the same time. In the other periods analyzed (freezing period in 2010, 2012, freezing periods in 2013 and 2014) water tension with values below pF = 1.8 was measured in the whole active layer. However, during thawing in 2012, over a period of 20 days, all three layers were saturated, but this time period was probably too short to cause mass movement.<sup>62</sup> Interestingly, from September 6 to October 31, 2010 (55 days), where pF values <1.8 were measured, this period should have been long enough to trigger solifluction. High soil moisture enhances solifluction processes, especially when soil moisture is above the liquid limit.<sup>63</sup> As already mentioned in the section on the freezing period and based on the stable and visible polygons,<sup>16,64</sup> it can be assumed that the threshold pF < 1.8 is not enough to trigger solifluction. The situation is different with a complete water saturation of pF = 0. However, complete water saturation in the active layer only occurred in October 2013 for 25 h at 20 and 35 cm depth. It cannot be ruled out that the soil had higher water tension values at a depth of 10 cm, as the pF<sub>1</sub>-sensor was no longer measuring at this time.

There might be further explanations for this phenomenon. (a) Regional climate is very important at this location and, due to the katabatic winds, it is dry and cold.<sup>24</sup> This may lead to less water accumulation in the active layer and thus to a more stable slope.<sup>55</sup> In addition, the vegetation cover, and thus water uptake and transpiration, prevent water accumulation in the active layer as well as

evaporation.<sup>19,20,65</sup> Furthermore, the vegetation cover has a binding effect on the near-surface soil, which is another stabilizing factor.<sup>40,66</sup> However, these explanations are not sufficient if there is complete water saturation ( $pF = 0$ ), despite vegetation cover.

(b) A second explanation for the stabilization of the slope are ice wedges and their surficial arrangement in polygonal networks themselves. Ice wedges with their solid ice represent obstacles for the water-saturated soil to move downslope.<sup>9</sup> During the freezing period we observed that for certain time periods  $pF$  values of 0 occurred in the lowest active layer depth for between 6.5 (2009) and 92 days (2012). They probably resulted from subsurface water runoff along the permafrost table.<sup>67</sup> However, this water encounters the ice wedges, which act as natural barriers downslope that are strong enough in this north-facing slope situation to create a stagnating effect.<sup>68</sup> As a result, the water cannot create an undisturbed flow path and completely run down the slope.<sup>12</sup> Moreover, the ice wedge troughs may act as hydrological drainage pathways to channel the water downslope instead of diffuse infiltration and saturation of the active layer.<sup>69,70</sup> Since the period with  $pF = 0$  is generally short at all depths (between 0 and 92 days), the dense root network of shrub tundra (vegetation coverage of 100%) can have a sufficient stabilizing effect.<sup>71,72</sup>

A similar phenomenon of stable ice wedge polygons in frozen sediments on steep slopes was observed in Spitsbergen.<sup>17</sup> The authors proposed limited frost heave and formation of ice segregation in combination with dry climate conditions as possible causes. This and our observation that the phases of water saturation in the active layer did not last long enough to trigger solifluction are supported by the dry and cold climate and the dense vegetation cover in the study area in West Greenland. In addition, the ice wedges within a polygon net may stabilize each other and form a natural barrier that prevents a direct runoff path downslope.<sup>69</sup>

However, this may change with ongoing climate change, which would result in more water being able to accumulate in the active layer over longer periods, increasing the depth of the active layer, and thus leading to solifluction processes in the future. As a result, the ice wedges would subside, which might lead to large-scale slope destabilization at the current rate of global warming. Note that the thawing potential of the permafrost in the region around Kangerlussuaq has been classified as high<sup>73</sup> and the scenario outlined above could occur in the coming decades.

#### 4.5 | Timing of the formation of organic matter-rich permafrost on slopes

The so far oldest radiocarbon age of about 8,050 cal BP from organic matter within the Umivit/Keglen moraines is from Lille Saltso (AAR-3507), which is located about 10 km southwest of the oldest radiocarbon age in the Sandflugtdalen (UtC-1987) of about 7,600 cal BP.<sup>26</sup> This east-west distance may be the cause of the younger age of the eastward UtC-1987 site in Sandflugtdalen. Since the UtC-1987 site is in a comparable location to the monitoring station in the

Umimallissuaq valley with respect to the recent ice margin, this age can be considered a better approximation for the maximum age for formation of periglacial phenomena in the Umimallissuaq valley than the age of AAR-3507. The oldest radiocarbon age from an Ah horizon (valley floor) of our study site in the Umimallissuaq valley so far is about 5,100 cal BP (Erl-19000 in Table 1).

Erl-16618 (from profile C11) yielded the oldest age from organic matter-rich permafrost in an ice wedge polygon at about 3,300 cal BP. This can be considered as the minimum age for the beginning of the accumulation of the organic matter-rich permafrost on this slope. Since the base of the permafrost on the slope was not assessed and the valley floor was already deglaciated at about 5,100 cal BP, permafrost accumulation could have already started at that time. This is supported by the age of about 4,600 cal BP (Erl-16614) from a buried A horizon in profile C13 located between the moraine and slope (see Table S1). However, it cannot be excluded that the onset of permafrost accumulation started earlier, that is from 7,600 cal BP (UtC-1987), as this site also lies within the Umivit/Keglen moraine.

Interestingly, the ~800 years younger age of MAL 12293, sampled in the same profile 80 cm above Erl-16618, indicates a constant upward growth of organic matter-rich permafrost on these slopes. This can be seen as a constant process caused by the katabatic winds transporting silty sediments to the slope<sup>24</sup> and the more or less seasonal accumulation of organic material. The maximum age for the ice wedge polygons on the slopes can be assumed to be about 5,000 years, at least if enough sediment had already been deposited to allow ice wedge formation.

## 5 | CONCLUSION

The current study presents hourly soil temperature and water saturation data from the active layer in the Umimallissuaq valley in West Greenland over 6 years and investigates the reason for the stable polygon networks on steep slopes found there.

It could be shown that the water content within the active layer was not high enough and phases of water saturation were not long enough during the measurement period to trigger slope movement and thus solifluction. The results indicate a direct connection between soil moisture tension and soil temperature, and show that there was no temporal overlap of water saturation at the three depths of the active layer. These effects of a generally low water saturation can be explained by the cold and dry climate and limited frost heave processes, a dense vegetation cover and root network, but also by a natural barrier effect of ice wedges, which prevent direct downslope runoff. From this we conclude that the ice wedge polygon networks on north-facing exposed slopes in West Greenland are currently stable and so is the active layer near the ice margin, especially where the katabatic winds are active. It is assumed that the stability of these north-facing slopes has existed for about 5,000 years. Therefore, and because of the continuous growth of the organic matter-rich permafrost on these slopes, the permafrost

and the ice wedges could also serve as a paleoenvironmental archive for this period.

However, the available data from a single soil measurement station provide only limited insight into the fragile environment of permafrost soils and ice wedge polygon networks. Moreover, it is as yet unknown how climate change will influence these complex systems. Annual mean temperature in West Greenland is expected to increase by 2.5–3°C for the RCP4.5 scenario and by 4.8–6.0°C for the RCP8.5 scenario, as well as an increase in precipitation of 20–30 and 30–80%, respectively, by the end of this century.<sup>74</sup> This may change the moisture regime toward longer periods of positive pore pressure, destabilization of ice wedge polygons, and mass movement and solifluction along north-facing slopes.

## AUTHOR CONTRIBUTIONS

PK designed the study and carried out fieldwork. KS analyzed the data and prepared graphs. KS prepared the manuscript with contributions from all coauthors.

## ACKNOWLEDGEMENTS

We thank all the students and colleagues who contributed to the fieldwork and the installation and maintenance of the station from 2009 to 2015, in particular Frank Baumann, Tobias Neder, Michael Müller, Christian Wolf, and Jessica Henkner. We also thank Isabelle Beutelspacher for her error analysis of the monitoring data. KS is greatly indebted to Dr Eugenia Schwarzkopf, who proofread the manuscript. We thank the two unknown reviewers for their helpful comments and contributions to the manuscript. Open Access funding enabled and organized by Projekt DEAL.

## CONFLICT OF INTEREST STATEMENT

The authors declare that they have no conflicts of interest.

## DATA AVAILABILITY STATEMENT

The data that support the findings of this study are available from the corresponding author upon reasonable request.

## ORCID

Katharina Schwarzkopf  <https://orcid.org/0000-0003-4541-260X>

Steffen Seitz  <https://orcid.org/0000-0003-4911-3906>

Michael Fritz  <https://orcid.org/0000-0003-4591-7325>

Thomas Scholten  <https://orcid.org/0000-0002-4875-2602>

Peter Kühn  <https://orcid.org/0000-0002-4417-5633>

## REFERENCES

- van Angelen JH, van den Broeke MR, Wouters B, Lenaerts JTM. Contemporary (1960–2012) evolution of the climate and surface mass balance of the Greenland ice sheet. *Surv Geophys*. 2014;35(5):1155–1174. doi:10.1007/s10712-013-9261-z
- Schaefer K, Lantuit H, Romanovsky VE, Schuur EAG, Witt R. The impact of the permafrost carbon feedback on global climate. *Environ Res Lett*. 2014;9(8):85003. doi:10.1088/1748-9326/9/8/085003
- Steffen W, Rockström J, Richardson K, et al. Trajectories of the earth system in the Anthropocene. *Proc Natl Acad Sci U S A*. 2018;115(33):8252–8259. doi:10.1073/pnas.1810141115
- Hollesen J, Elberling B, Jansson PE. Future active layer dynamics and carbon dioxide production from thawing permafrost layers in North-east Greenland. *Glob Chang Biol*. 2011;17(2):911–926. doi:10.1111/j.1365-2486.2010.02256.x
- Byun E, Yang J-W, Kim Y, Ahn J. Trapped greenhouse gases in the permafrost active layer: preliminary results for methane peaks in vertical profiles of frozen Alaskan soil cores. *Permafr Periglac Proc*. 2017;28(2):477–484. doi:10.1002/ppp.1935
- James SR, Knox HA, Abbott RE, Panning MP, Screamon EJ. Insights into permafrost and seasonal active-layer dynamics from ambient seismic noise monitoring. *Case Rep Med*. 2019;124(7):1798–1816. doi:10.1029/2019JF005051
- Lenton TM. Arctic climate tipping points. *Ambio*. 2012;41(1):10–22. doi:10.1007/s13280-011-0221-x
- Brown J, Hinkel KM, Nelson FE. The circumpolar active layer monitoring (calm) program: research designs and initial results 1. *Polar Geogr*. 2000;24(3):166–258. doi:10.1080/10889370009377698
- Burn CR, Lewkowicz AG, Wilson MA. Long-term field measurements of climate-induced thaw subsidence above ice wedges on hillslopes, western Arctic Canada. *Permafr Periglac Proc*. 2021;32(2):261–276. doi:10.1002/ppp.2113
- Christiansen HH, Matsuoka N, Watanabe T. Progress in understanding the dynamics, internal structure and Palaeoenvironmental potential of ice wedges and sand wedges. *Permafr Periglac Proc*. 2016;27(4):365–376. doi:10.1002/ppp.1920
- O'Neill HB, Christiansen HH. Detection of ice wedge cracking in permafrost using miniature accelerometers. *Case Rep Med*. 2018;123(4):642–657. doi:10.1002/2017JF004343
- Jorgenson MT, Kanevskiy M, Shur Y, et al. Role of ground ice dynamics and ecological feedbacks in recent ice wedge degradation and stabilization. *Case Rep Med*. 2015;120(11):2280–2297. doi:10.1002/2015JF003602
- Gunn B, Warren G. (1962): Geology of Victoria land between Mawson and Mulock glaciers, Antarctica.
- Selby MJ. Slopes and their development in an ice-free, arid area of Antarctica. *Geogr Ann Ser B*. 1971;53(3–4):235–245. doi:10.1080/04353676.1971.11879849
- Mackay JR. Some observations on the growth and deformation of epigenetic, syngenetic and anti-syngenetic ice wedges. *Permafr Periglac Proc*. 1990;1(1):15–29. doi:10.1002/ppp.3430010104
- Mackay JR. Ice wedges on hillslopes and landform evolution in the late Quaternary, western Arctic coast, Canada. *Can J Earth Sci*. 1995;32(8):1093–1105. doi:10.1139/e95-091
- Sørbel L, Tolgensbakk J. Ice-wedge polygons and solifluction in the Adventdalen area, Spitsbergen, Svalbard. *Norsk Geografisk Tidsskrift - Norwegian J Geog*. 2002;56(2):62–66. doi:10.1080/002919502760056369
- Lewkowicz AG, Harris C. Frequency and magnitude of active-layer detachment failures in discontinuous and continuous permafrost, northern Canada. *Permafr Periglac Proc*. 2005;16(1):115–130. doi:10.1002/ppp.522
- Matsuoka N. Solifluction rates, processes and landforms: a global review. *Earth Sci Rev*. 2001;55(1–2):107–134. doi:10.1016/S0012-8252(01)00057-5
- Hjort J. Which environmental factors determine recent cryoturbation and Solifluction activity in a subarctic landscape? A comparison between active and inactive features. *Permafr Periglac Proc*. 2014;25(2):136–143. doi:10.1002/ppp.1808
- Henkner J, Scholten T, Kühn P. Soil organic carbon stocks in permafrost-affected soils in West Greenland. *Geoderma*. 2016;282:147–159. doi:10.1016/j.geoderma.2016.06.021
- Nielsen, A. B. (2010) Present conditions in Greenland and the Kangerlussuaq area. Working Report. In Posiva, Oulu, 1–75 pp.
- Walker, D. A.; Raynolds, Martha K.; Maier, Hilmar A.; Trahan, Natalie G. (2003): Circumpolar Arctic vegetation. Anchorage, Alaska,

- Fairbanks: U.S. Fish and Wildlife Service; Geophysical Institute Map Office [distributor] (Conservation of Arctic Flora and Fauna [CAFF] map, no. 1).
24. Müller M, Thiel C, Kühn P. Holocene palaeosols and aeolian activities in the Umimallissuaq valley, West Greenland. *The Holocene*. 2016; 26(7):1149-1161. doi:10.1177/09596836166632885
  25. Young NE, Briner JP, Miller GH, et al. Deglaciation of the Greenland and Laurentide ice sheets interrupted by glacier advance during abrupt coolings. *Quat Sci Rev*. 2020;229:106091. doi:10.1016/j.quascirev.2019.106091
  26. van Tatenhove FGM, van der Meer JJM, Koster EA. Implications for deglaciation chronology from new AMS age determinations in central West Greenland. *Quatern Res*. 1996;45(3):245-253. doi:10.1006/qres.1996.0025
  27. Bennike O. Palaeoecological studies of Holocene lake sediments from West Greenland. *Palaeogeogr Palaeoclimatol Palaeoecol*. 2000;155(3-4): 285, 304-304. doi:10.1016/S0031-0182(99)00121-2
  28. Amelung W, Blume H-P, Fleige H, et al. *Scheffer/Schachtschabel Lehrbuch der Bodenkunde*. Berlin, Heidelberg: Springer Berlin Heidelberg; 2018.
  29. Wickham H. *ggplot2: Elegant graphics for data analysis*. New York: Springer-Verlag; 2016. doi:10.1007/978-3-319-24277-4
  30. Wickham H, Averick M, Bryan J, et al. Welcome to the tidyverse. *J Open S Softw*. 2019;4(43):1686. doi:10.21105/joss.01686
  31. Henriksen N. *Geological history of Greenland. Four billion years of earth evolution*. København: Geological Survey of Denmark and Greenland; 2008.
  32. Bronk Ramsey C. Bayesian analysis of radiocarbon dates. *Radiocarbon*. 2009;51(1):337-360. doi:10.1017/S0033822200033865
  33. Reimer PJ, Austin WEN, Bard E, et al. The IntCal20 northern hemisphere radiocarbon age calibration curve (0-55 cal kBP). *Radiocarbon*. 2020;62(4):725-757. doi:10.1017/RDC.2020.41
  34. Elberling B, Tamstorf MP, Michelsen A, et al. Soil and Plant Community-Characteristics and Dynamics at Zackenberg. In: *High-Arctic ecosystem dynamics in a changing climate*. Vol.40. Elsevier (Advances in Ecological Research); 2008:223-248.
  35. Beutelpacher I. *Zeitreihenanalyse von Bodentemperatur und Bodenfeuchte der Auftauzone in Westgrönland von 2009 bis 2015*. BSc Thesis. University of Tübingen; 2018:65.
  36. Oh S, Lu N. Slope stability analysis under unsaturated conditions: case studies of rainfall-induced failure of cut slopes. *Eng Geology*. 2015; 184:96-103. doi:10.1016/j.enggeo.2014.11.007
  37. White JA, Singham DI. Slope stability assessment using stochastic rainfall simulation. *Procedia Comput Sci*. 2012;9:699-706. doi:10.1016/j.procs.2012.04.075
  38. Fox GA, Chu-Agor M, Librada; Wilson, Glenn V. Erosion of noncohesive sediment by ground water seepage: Lysimeter experiments and stability modeling. *Soil Sci Soc Am J*. 2007;71(6):1822-1830. doi:10.2136/sssaj2007.0090
  39. Bordoni M, Valentino R, Meisina C, Bittelli M, Chersich S. A simplified approach to assess the soil saturation degree and stability of a representative slope affected by shallow landslides in Oltrepò Pavese (Italy). *Geosciences*. 2018;8(12):472. doi:10.3390/geosciences8120472
  40. Genxu W, Guangsheng L, Chunjie L, Yan Y. The variability of soil thermal and hydrological dynamics with vegetation cover in a permafrost region. *Agric for Meteorol*. 2012;162-163:44-57. doi:10.1016/j.agrformet.2012.04.006
  41. Gonzalez-Ollauri A, Mickovski SB. Hydrological effect of vegetation against rainfall-induced landslides. *J Hydrol*. 2017;549:374-387. doi:10.1016/j.jhydrol.2017.04.014
  42. Liu HW, Feng S, Ng CWW. Analytical analysis of hydraulic effect of vegetation on shallow slope stability with different root architectures. *Comput Geotechnics*. 2016;80:115-120. doi:10.1016/j.compgeo.2016.06.006
  43. Hallinger M, Manthey M, Wilmking M. Establishing a missing link: warm summers and winter snow cover promote shrub expansion into alpine tundra in Scandinavia. *New Phytol*. 2010;186(4):890-899. doi:10.1111/j.1469-8137.2010.03223.x
  44. Callaghan TV, Johansson M, Brown RD, et al. The changing face of Arctic snow cover: a synthesis of observed and projected changes. *Ambio*. 2011;40(S1):17-31. doi:10.1007/s13280-011-0212-y
  45. Jespersen RG, Leffler AJ, Oberbauer SF, Welker JM. Arctic plant eco-physiology and water source utilization in response to altered snow: isotopic ( $\delta^{18}\text{O}$  and  $\delta^2\text{H}$ ) evidence for meltwater subsidies to deciduous shrubs. *Oecologia*. 2018;187(4):1009-1023. doi:10.1007/s00442-018-4196-1
  46. Pavlyk VG, Kutnyi AM, Kalnyk OP. GEODYNAMICS. In: JGD, ed. 2019 (2[27]); 2019:16-23. doi:10.23939/jgd2019.02.016
  47. Mohammed AA, Kurylyk BL, Cey EE, Hayashi M. Snowmelt infiltration and macropore flow in frozen soils: overview, knowledge gaps, and a conceptual framework. *Vadose Zone J*. 2018;17(1):180084. doi:10.2136/vzj2018.04.0084
  48. Kelleners TJ, Norton JB. Determining water retention in seasonally frozen soils using hydra impedance sensors. *Soil Sci Soc Am J*. 2012; 76(1):36-50. doi:10.2136/sssaj2011.0222
  49. Wan X, Lai Y, Wang C. Experimental study on the freezing temperatures of saline silty soils. *Permafr Periglac Proc*. 2015;26(2):175-187. doi:10.1002/ppp.1837
  50. Henkemans E, Frape SK, Ruskeeniemi T, Anderson NJ, Hobbs M. A landscape-isotopic approach to the geochemical characterization of lakes in the Kangerlussuaq region, West Greenland. *Arctic Antarctic Alpine Res*. 2018;50(1):S100018. doi:10.1080/15230430.2017.1420863
  51. Walvoord MA, Kurylyk BL. Hydrologic impacts of thawing permafrost-a review. *Vadose Zone J*. 2016;15(6):vzj2016.01.0010. doi:10.2136/vzj2016.01.0010
  52. Lawrence DM, Koven CD, Swenson SC, Riley WJ, Slater AG. Permafrost thaw and resulting soil moisture changes regulate projected high-latitude CO<sub>2</sub> and CH<sub>4</sub> emissions. *Environ Res Lett*. 2015;10(9): 94011. doi:10.1088/1748-9326/10/9/094011
  53. Radville L, Post E, Eissenstat DM. On the sensitivity of root and leaf phenology to warming in the Arctic. *Arctic Antarctic Alpine Res*. 2018; 50(1):S100020. doi:10.1080/15230430.2017.1414457
  54. Gadi VK, Hussain R, Bordoloi S, et al. Relating stomatal conductance and surface area with evapotranspiration induced suction in a heterogeneous grass cover. *J Hydrol*. 2019;568:867-876. doi:10.1016/j.jhydrol.2018.11.048
  55. Sattler K, Elwood D, Hendry MT, et al. Quantifying the contribution of matric suction on changes in stability and displacement rate of a translational landslide in glaciolacustrine clay. *Landslides*. 2021;18(5): 1675-1689. doi:10.1007/s10346-020-01611-3
  56. Keegan KM, Albert MR, McConnell JR, Baker I. Climate change and forest fires synergistically drive widespread melt events of the Greenland ice sheet. *Proc Natl Acad Sci U S A*. 2014;111(22):7964-7967. doi:10.1073/pnas.1405397111
  57. Pries H, Caitlin E, Schuur EAG, Vogel JG, Natali SM. Moisture drives surface decomposition in thawing tundra. *Eur J Vasc Endovasc Surg*. 2013;118(3):1133-1143. doi:10.1002/jgrg.20089
  58. Zhang X, Wu Y, Zhai E, Ye P. Coupling analysis of the heat-water dynamics and frozen depth in a seasonally frozen zone. *J Hydrol*. 2021;593:125603. doi:10.1016/j.jhydrol.2020.125603
  59. Akerman HJ. Relations between slow slope processes and active-layer thickness 1972-2002, Kapp Linné, Svalbard. *Norsk Geogr Tidsskr - Norwegian J Geog*. 2005;59(2):116-128. doi:10.1080/00291950510038386
  60. Matsuoka N. Solifluction and mudflow on a limestone periglacial slope in the Swiss Alps: 14 years of monitoring. *Permafr Periglac Proc*. 2010;21(3):219-240. doi:10.1002/ppp.678

61. Harris C, Smith JS, Davies MCR, Rea B. An investigation of periglacial slope stability in relation to soil properties based on physical modelling in the geotechnical centrifuge. *Geomorphology*. 2008b;93(3-4):437-459. doi:[10.1016/j.geomorph.2007.03.009](https://doi.org/10.1016/j.geomorph.2007.03.009)
62. Harris C, Kern-Luetsch M, Murton J, Font M, Davies M, Smith F. Solifluction processes on permafrost and non-permafrost slopes: results of a large-scale laboratory simulation. *Permafrost Periglacial Proc*. 2008a;19(4):359-378. doi:[10.1002/ppp.630](https://doi.org/10.1002/ppp.630)
63. Kinnard C, Lewkowicz AG. Movement, moisture and thermal conditions at a turf-banked solifluction lobe, Kluane range, Yukon territory, Canada. *Permafrost Periglacial Proc*. 2005;16(3):261-275. doi:[10.1002/ppp.530](https://doi.org/10.1002/ppp.530)
64. Streletskiy DA, Shiklomanov NI, Little JD, et al. Thaw subsidence in undisturbed tundra landscapes, Barrow, Alaska, 1962-2015. *Permafrost Periglacial Proc*. 2017;28(3):566-572. doi:[10.1002/ppp.1918](https://doi.org/10.1002/ppp.1918)
65. Jaesche P, Veit H, Huwe B. Snow cover and soil moisture controls on solifluction in an area of seasonal frost, eastern Alps. *Permafrost Periglacial Proc*. 2003;14(4):399-410. doi:[10.1002/ppp.471](https://doi.org/10.1002/ppp.471)
66. Matsuoka N. Climate and material controls on periglacial soil processes: toward improving periglacial climate indicators. *Quatern Res*. 2011;75(2):356-365. doi:[10.1016/j.yqres.2010.12.014](https://doi.org/10.1016/j.yqres.2010.12.014)
67. Shiklomanov NI, Streletskiy DA, Little JD, Nelson FE. Isotropic thaw subsidence in undisturbed permafrost landscapes. *Geophys Res Lett*. 2013;40(24):6356-6361. doi:[10.1002/2013GL058295](https://doi.org/10.1002/2013GL058295)
68. Kanevskiy M, Shur Y, Jorgenson T, et al. Degradation and stabilization of ice wedges: implications for assessing risk of thermokarst in northern Alaska. *Geomorphology*. 2017;297:20-42. doi:[10.1016/j.geomorph.2017.09.001](https://doi.org/10.1016/j.geomorph.2017.09.001)
69. Koch JC, Jorgenson MT, Wickland KP, Kanevskiy M, Striegl R. Ice wedge degradation and stabilization impact water budgets and nutrient cycling in Arctic trough ponds. *Eur J Vasc Endovasc Surg*. 2018;123(8):2604-2616. doi:[10.1029/2018JG004528](https://doi.org/10.1029/2018JG004528)
70. Wales NA, Gomez-Velez JD, Newman BD, et al. Understanding the relative importance of vertical and horizontal flow in ice-wedge polygons. *Hydrol Earth Syst Sci*. 2020;24(3):1109-1129. doi:[10.5194/hess-24-1109-2020](https://doi.org/10.5194/hess-24-1109-2020)
71. Cray HA, Pollard WH. Vegetation recovery patterns following permafrost disturbance in a low Arctic setting: case study of Herschel Island, Yukon, Canada. *Arctic Antarctic Alpine Res*. 2015;47(1):99-113. doi:[10.1657/AAAR0013-076](https://doi.org/10.1657/AAAR0013-076)
72. Forbes BC, Ebersole JJ, Strandberg B. Anthropogenic disturbance and patch dynamics in circumpolar Arctic ecosystems. *Conserv Biol*. 2001;15(4):954-969. doi:[10.1046/j.1523-1739.2001.015004954.x](https://doi.org/10.1046/j.1523-1739.2001.015004954.x)
73. Daanen RP, Ingeman-Nielsen T, Marchenko SS, et al. Permafrost degradation risk zone assessment using simulation models. *Cryosphere*. 2011;5(4):1043-1056. doi:[10.5194/tc-5-1043-2011](https://doi.org/10.5194/tc-5-1043-2011)
74. Boberg F, Langen PL, Mottram RH, Christensen JH, Olesen M. 21st-century climate change around Kangerlussuaq, West Greenland: from the ice sheet to the shores of Davis Strait. *Arct, Antarct Alpine Res*. 2018;50(1):S100006. doi:[10.1080/15230430.2017.1420862](https://doi.org/10.1080/15230430.2017.1420862)
75. IUSS Working Group WRB. *World Reference Base for soil resources. International soil classification system for naming soils and creating legends for soil maps*. 4th edition. Vienna, Austria: International Union of Soil Sciences (IUSS); 2022.

## SUPPORTING INFORMATION

Additional supporting information can be found online in the Supporting Information section at the end of this article.

**How to cite this article:** Schwarzkopf K, Seitz S, Fritz M, Scholten T, Kühn P. Ice wedge polygon stability on steep slopes in West Greenland related to temperature and moisture dynamics of the active layer. *Permafrost and Periglacial Process*. 2023;34(2):194-207. doi:[10.1002/ppp.2181](https://doi.org/10.1002/ppp.2181)